

**Technical Report 1657**

June 1994

# **Metal/Hydrogen Energy Storage: Selected Technical Issues**

P. A. Mosier-Boss

S. J. Szpak

## SUMMARY

### OBJECTIVE

The objective is to illustrate a rational approach for modeling and characterizing porous electrodes. Although we selected the metal hydride system for this purpose, such an approach is applicable to other systems as well and is an example of current trends in the development of electrochemical cells.

### RESULTS AND CONCLUSIONS

With an increased awareness of the environment and how human activities impact the ecosystem, current trends in the development of energy storage systems are to employ less hazardous material. Consequently, recent years have witnessed increased interest and activity in the development of the "hydrogen economy." There has been particular emphasis in using hydrogen as the fuel in energy generating devices such as hydrogen/oxygen fuel cells or as rechargeable batteries in which the negative electrode contains hydrogen absorbed in an alloy. These metal hydride systems show a great deal of promise due to their high theoretical energy and power densities, rechargeability, and potential broad range applications. Although the first intermetallic hydride was developed thirty years ago and despite construction of the first prototype metal hydrogen electrode twenty years ago, metal hydrogen electrodes still experience many shortcomings. These include high cost of alloys, poor hydrogen storage capabilities, difficult activation, pyrophoricity, problems of impurities, thermodynamic instabilities, and corrosion in alkaline media.

Experience has shown that before a battery system is ready for full-scale applications, a logical progression of transitions through the R&D cycle must be pursued. In particular, modeling contributes significantly to understanding battery operation. The premise of modeling is that the description of electrode operation can be reduced to a set of precise mathematical statements whose solution serves as a guide for the selection and design procedures to meet performance requirements. A blueprint for an effective R&D program is presented which (1) emphasizes a rational transition from 6.1 to 6.2 and (2) relies on the synergistic effects arising from merging theoretical concepts with the requirements of practical devices.



# CONTENTS

<b>1</b>	<b>INTRODUCTION</b> .....	<b>1</b>
<b>2</b>	<b>CURRENT RESEARCH IN ELECTRODE DEVELOPMENT</b> .....	<b>1</b>
2.1	ELECTRODE MATERIAL—AB <sub>2</sub> AND AB <sub>5</sub> ALLOYS .....	2
2.2	ELECTRODE PREPARATION .....	2
<b>3</b>	<b>PHYSICAL PROPERTIES OF METAL HYDRIDE SYSTEMS</b> .....	<b>3</b>
3.1	KINETICS OF SORPTION/DESORPTION OF HYDROGEN .....	3
3.1.1	Hydrogen Sorption from Gas Phase .....	3
3.1.2	Hydrogen Sorption in Electrochemical Systems .....	3
3.2	THERMODYNAMICS OF SORPTION .....	5
3.2.1	Chemical Potential of Absorbed Hydrogen .....	5
3.2.2	Chemical Potential of Hydrogen in the Interphase .....	5
<b>4</b>	<b>TECHNOLOGY ISSUES</b> .....	<b>5</b>
4.1	THEORETICAL ASPECTS .....	6
4.1.1	Review of MH Electrode Modeling .....	6
4.1.2	Limitations of Current Models .....	6
4.2	SPECIFIC TASKS FOR MODELING .....	8
4.2.1	Development of Formalism for the MH Electrode .....	8
4.3	EXPERIMENTAL ASPECTS: MODEL CONSTRUCTION AND VERIFICATION .....	11
4.3.1	Simulations .....	11
4.3.2	Examination of the Electrode/Electrolyte Interphase .....	15
4.3.3	Experimental Cell to Monitor Hydrogen Sorption .....	16
<b>5</b>	<b>CONCLUDING REMARKS</b> .....	<b>17</b>
<b>6</b>	<b>SYMBOLS AND CHEMICAL EQUATIONS USED TO DERIVE EXPRESSIONS IN TABLE I</b> .....	<b>17</b>
6.1	LIST OF SYMBOLS USED IN EQUATIONS IN TABLE I .....	17
6.2	REACTIONS CONSIDERED IN DERIVING EQUATIONS IN TABLE I .....	19
<b>7</b>	<b>REFERENCES</b> .....	<b>19</b>

## Figures

1.	Schematic representation of an interphase for a hydrogen absorbing metal (fluxes included). (a) Adsorption plane; (t) charge transfer plane; (l) lattice .....	4
2.	One-dimensional model of a porous structure showing a, b subsystems .....	11
3.	Schematic derivation of single-pore analog cell through successive degrees of abstraction: A real electrode consisting of interconnected pores and bonded particles; B, idealized abstraction of A, retaining tortuous pores, but pores are no longer interconnected; C, further abstraction where pores pass straight through the electrodes (tortuosity factor = 1); D, section through the cell, shown as an abstraction and as the analog single-pore cell. ....	12

4.	Experimental cell assembly. Lower right: details of holder construction, electrical connections, and positioning of segmented electrode. Upper left: construction of segmented electrode showing vapor deposited silver on a glass substrate. The shaded area is a U-shaped Teflon tape, 60 mm thick .....	13
5.	Development of concentration gradients in an experimental cell, similar to that shown in Figure 4, as displayed with the aid of a Watson interference objective. Electrode reaction: ; galvanostatic conditions $j = 10 \text{ mA cm}^{-2}$ ; distance $x = 0.3 \text{ cm}$ ; the time between exposures is 60 s .....	14
6.	Electrolytic cell for the examination of an electrode surface by Nomarski optics. A = Pt counter electrode; B = Cu wire spotwelded to Pd electrode; C = etched Pd surface; D = Mylar film .....	15
7.	Design of the experimental cell. T1 and T2 refer to the temperatures of the MH electrode and solution, respectively .....	16

### Tables

1.	Summary of governing equations for Li/SOCl <sub>2</sub> cells. (Adapted from Tsaui and Pollard, 1984a and 1984b). List of symbols and reaction equations for Li/SOCl <sub>2</sub> electroreduction are found in sections 6.1 and 6.2, respectively .....	7
----	--	---

# 1. INTRODUCTION

With an increased awareness of the environment and how human activities impact the ecosystem, current trends in the development of energy storage systems are to employ less hazardous materials. Consequently, recent years have witnessed increased interest and activity in the development of the "hydrogen economy." There has been particular emphasis in using hydrogen as the fuel in energy generating devices such as hydrogen-oxygen fuel cells or as rechargeable batteries in which the negative electrode contains hydrogen absorbed in an alloy. In June 1992, at Argonne National Laboratory, DOE sponsored a workshop to develop a research strategy for a new program entitled "Advanced Battery Technology Research and Development" (US Department of Energy, 1992). This workshop focused on batteries for the consumer market. A notable feature of the discussions was the emphasis placed on the area of rechargeable batteries. Among the many systems discussed, rechargeable batteries based on zinc, lithium, and metal hydride negative electrodes and nickel-oxide positive electrodes were considered leading candidates to command a large share of the battery market.

Experience has shown that before a battery system is ready for full-scale applications, a logical progression of transitions through the R&D cycle must be pursued (Szpak and Smith, 1990). In organizing this report, we emphasize the role of modeling since it contributes significantly to understanding battery operation. The premise of modeling is that the description of electrode operation can be reduced to a set of precise mathematical statements whose solution serves as a guide for the selection and design procedures to meet performance requirements. The objective of this report is to provide a guide for the development and optimization of the performance envelope of a battery for a given application and emphasizes a rational transition from 6.1 to 6.2. A blueprint for an effective R & D program is presented which relies on the synergistic effects arising from merging theoretical concepts with the requirements of practical devices.

## 2. CURRENT RESEARCH IN ELECTRODE DEVELOPMENT

Nickel/metal hydride, Ni/MH, systems show a great deal of promise due to their high theoretical energy and power densities, rechargeability, and potential broad range applications. Research activities in the construction and characterization of metal hydrogen electrodes were discussed at the International Symposium on Metal-Hydrogen Systems in Uppsala, Sweden (June 8–12, 1992). Although the first intermetallic hydride was developed thirty years ago and despite construction of the first prototype metal hydrogen electrode twenty years ago, metal hydrogen electrodes still experience many shortcomings. These include high cost of alloys, poor hydrogen storage capabilities, difficult activation, pyrophoricity, problems of impurities, thermodynamic instabilities, and corrosion in alkaline media. In reviewing the progress, or lack thereof, in the field of metal hydrides, Suda and Sandrock (1992) concluded that new and radical changes in thinking and approach were required to overcome the difficulties encountered.

The renewed interest in Ni/MH systems is also evident from the topics presented at the October 1993 meeting of the Electrochemical Society held in New Orleans, Louisiana. Several papers dealt with the role of the interphase in H sorption. For example, Ohnishi et al. (1993) reported that the electrochemical behavior of the MH electrode is dependent upon the surface characteristics rather than bulk properties while the effect of surface composition on sorption of hydrogen from both gaseous and liquid phases was discussed by Florino et al. (Florino, Konstadinis, Opila, & Fang, 1993). The later noted that MgO affected H sorption but could find no correlation between the film composition

and bulk stability. Similarly, Ciureanu et al. (1993), employing both electrochemical (cyclic voltammetry and impedance) and physical methods (X-ray diffraction, Auger spectroscopy), concluded that the cell behavior was primarily governed by the interphase. Desilvestro, Reymond, Larcin, and Ruetschi (1993) in collaboration with Prof. Schlappbach, a noted researcher of *MH* systems, examined the morphological and structural changes of *MH* electrodes by SEM, X-ray diffraction, and ESCA techniques. Modeling of the discharge cycle; i.e., modeling of the hydrogen supply to the reaction surface, has been discussed by Viitanen (1992, 1993) and Luo et al. (Luo, Johnson, Feldberg, & Reilly, 1993). In the latter, discharge kinetics were taken into account.

Modeling of metal hydride electrodes requires the formulation of mathematical expressions that describe the transport processes within and between both the electrolyte and the hydrogen absorbing material. Data must be acquired which will aid in the construction and verification of the model. Finally, factors that affect hydrogen sorption must be examined.

## 2.1 ELECTRODE MATERIAL— $AB_2$ AND $AB_5$ ALLOYS

There are two classes of metal hydride alloys employed as negative electrodes, the  $AB_2$  ( $ZrNi_2$  where *Ni* can be substituted by *V*, *Cr*, or *Mn*) and  $AB_5$  ( $LaNi_5$ ) alloys. Both classes of alloys include many additional metal components which improve performance, life, and self-discharge. With the passage of time, what at first was a simple binary alloy electrode has now become a complex, multi-component alloy system.

Although the  $AB_2$  compounds, such as  $ZrNi_2$ , show reversible hydrogen absorption which is larger than that of  $LaNi_5$ , they exhibit poorer charge and mass transfer kinetics (Zeutzel, 1992). For the absorption-desorption of hydrogen from the gas phase for both the  $AB_2$  and  $AB_5$  alloys, the plateau pressures fall between  $10^{-2}$  and 0.5 atm at 20°C with capacities of 1.0–1.3 *H/Me*. This translates into electrochemical capacities in the range of 350 – 400 mA/g (Canet et al., 1992). The general composition of  $AB_5$ -type hydrogen absorbing alloys used for battery applications is  $Mm(Ni - Co - Mn - F)_x$ , with  $4.5 < x < 4.8$ , where *Mm* denotes the “mischmetal” (a mixture of lanthanide metals). Depending upon the battery application, these  $AB_5$ -type alloys are modified by the addition of *Mo*, *B*, *Ta*, *W*, and *Zr*. For use as electrode materials in the construction of batteries, these alloys must exhibit corrosion resistance and high reactivity for the charge transfer reaction in alkaline solutions as well as high hydrogen absorption capacities (Ise et al., 1992). The  $AB_5$  compounds, in particular  $LaNi_5$  and  $LaCo_5$ , are not stable in alkaline electrolytes. Substitution of small amounts of either *Ca* or *Ni* for *Co* has been found to improve the stability of  $LaCo_5$ . This stability has been attributed to the production of a multiphase material. The problem of instability in alkaline media has also been solved by making the *x*-component of the  $AB_x$  alloy greater than 5. Besides providing long term stability, this latter modification assures higher catalytic activity and the alloys are easier to prepare (Kanda et al., 1992). Today, quality controlled electrode materials are available from Gesellschaft fuer Elektrometallurgie m.b.H. Sparte Innovation, Hoefener Strasse, D-8500 Nuernberg 80 (Friedrich, 1992). The availability of “made to order” materials greatly accelerates construction of electrodes and model verification.

## 2.2 ELECTRODE PREPARATION

Preparation of the electrode structure is, empirically, one of the most important tasks associated with the development of practical batteries. Typically, the metal hydride electrode for a sealed *Ni/MH* battery consists of a multicomponent powder (50  $\mu\text{m}$   $MmNi_5$  particle size) encapsulated with a porous 0.5  $\mu\text{m}$  *Ni* layer deposited by electroless plating. These particles are placed onto a “foamed” *Ni* matrix. Using electrodes of this design, AA size batteries with 1.0–1.2 AH at 0.2 C rate were built. This is equivalent to 60 Wh/kg or 170 Wh/l. Charge retention was found to be 70% after 28 days of

storage at room temperature (Yunshi et al., 1992). A somewhat different electrode preparation was described by Kuriyama et al. (1992). They used three methods of preparing electrodes of an  $MmNi_{3.5}Co_{0.7}Al_{0.8}$  alloy. The particle size of the alloy ranged between 0.12 and 0.15 mm. In preparation A, the alloy particles were coated, by an unspecified process, with 20 wt% *Cu* and 10 wt% perfluororesin. The alloy was mixed with 20 wt% and 10 wt% perfluororesin to yield preparation B. In preparation C, the alloy particles were simply mixed with 10 wt% perfluororesin. Each mixture was compacted into a pellet and provided with a current collector. Impedance spectra, from 0.5 mHz to 10 kHz, were recorded for each electrode at various discharge depths and temperatures under open circuit conditions after 20 and 440 cycles for preparation A, after 20 and 410 cycles for B, and after 20 and 130 cycles for C. Electrochemical impedance spectroscopy provides a means to study deterioration mechanisms of porous electrodes. The results of Kuriyama et al. (1992) indicated that the deterioration of C resulted from poor contact between the current collector and the pellet as well as between the alloy particles themselves. Furthermore, the *Cu* layer on the alloy particles used in preparation A was found to be effective in preserving good electrical contact in the electrode.

### 3. PHYSICAL PROPERTIES OF METAL HYDRIDE SYSTEMS

#### 3.1 KINETICS OF SORPTION/DESORPTION OF HYDROGEN

Another important issue in developing MH electrodes concerns the rate at which an  $AB_2$  or  $AB_5$  alloy can absorb hydrogen generated either electrochemically or supplied from the gas phase. At first glance, the reported data on the subject reveal a great deal of discrepancy which can be attributed to both the complexity of the reaction kinetics and the transfer path. This interpretation is based upon the fact that the rate constants for absorption and desorption of hydrogen are normally reported under the condition of constant temperature. Since absorption-desorption processes are either endo- or exothermic, this condition is difficult to satisfy.

##### 3.1.1 Hydrogen Sorption from Gas Phase

The majority of the studies dealing with the absorption of hydrogen have been conducted from the gas phase. Dantzer et al. (Dantzer, Pons, Guillot, & Cai, 1992) and Cimato et al. (Cimato, Zhang, Goudy, & Singleton, 1992) reported that  $LaNi_5$  absorbs hydrogen slower than  $LaNi_{4.7}Al_{0.3}$ . This observation was confirmed by Uchito and Hoshimoto (1992), who attributed the difference to surface activity promoted by the presence of *Al*-oxides. Stauffer, Ezzehar, and Dreysse (1992) reported on an interesting observation of hydrogen clustering near the metallic surface. Their results indicated that surface activity is very specific as shown by the differences between *Ni* and *Pd* surfaces. Besides the existence of higher hydrogen concentrations at the *Pd*-surface, there are two energetic states of adsorbed hydrogen. This latter observation has support from recent voltammetric results obtained for the *Pd*/ $H_2O$  system (Szpak, Mosier-Boss, Scharber, & Smith, 1992; Szpak, Mosier-Boss, Gabriel, & Smith, 1994).

##### 3.1.2 Hydrogen Sorption in Electrochemical Systems

Due to the non-autonomous character of the electrode/electrolyte interphase, a substantially greater number of factors affect the sorption process than in the gas phase. An interphase region is formed whenever an electrode is in contact with an electrolyte. In the simplest case, the interphase region takes the form of the electrical double layer. In the more complex cases and, in particular, during the charge transfer reaction, it consists of layers, each associated with a participating elementary process.

In this representation, the interphase region is an open system in which a number of consecutive processes takes place, of which the slowest one determines the rate. These processes include transport of the reactants from the bulk to the electrode surface by diffusion, adsorption on the electrode surface, charge transfer, desorption of the reaction products, followed by transport of the reaction products away from the electrode surface. In a discharging battery, these same processes occur; however, in a battery the electrons ultimately flow into an external circuit where the electrical work is delivered.

In the negative electrode, the relevant processes during discharge of the *Ni – MH* battery occur in a multiphase environment—gas, liquid, and solid. Due to the hydrogen absorption capabilities of the alloy making up the negative electrode; the electrode itself is often a multiphase system. Transport across such an interphase is a dynamic set of consecutive processes as illustrated in Figure 1. The central role of the interphase in transport of electrochemically generated hydrogen into the electrode interior has been discussed recently (Szpak, Mosier–Boss, Scharber, & Smith, 1992; Szpak, Mosier–Boss, Gabriel, & Smith, 1994) and the non-autonomous character of the interphase was stressed. It was shown that the interphase is an active element and that its properties are determined by those of the contacting phases, i.e., the electrode interior as well as the electrolyte. The role of the interphase may vary from that of an inhibitor to an accelerator of both charge transfer and molecular transport. (Ohnishi et al., 1993; Ciureanu et al., 1993; Dantzer, Pons, Guillot, & Cai, 1992; Cimato, Zhang, Goudy, & Singleton, 1992). This concept, although not explicitly stated, was implied in the discussion of hydrogen absorption from the gas phase (Stauffer, Ezzehar, & Dreysse, 1992) where it was shown that small metal alloy clusters absorb more hydrogen via a mechanism that becomes inoperative as the cluster size increases. The interphase may be modified in the course of battery operation, especially as a result of cycling. For example, Hasegawa et al. (1992) observed the development of an interphase consisting of a transition metal layer which, upon cycling, improved cell performance.

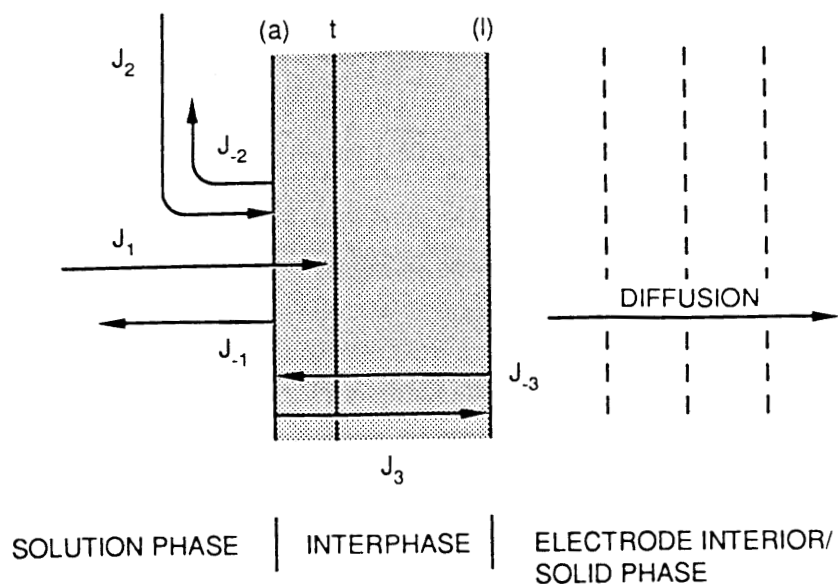


**Figure 1.** Schematic representation of an interphase for a hydrogen absorbing metal (fluxes included). (a) Adsorption plane; (t) charge transfer plane; (l) lattice.

## 3.2 THERMODYNAMICS OF SORPTION

Recently, thermodynamic and kinetic factors in cathodic  $H$ -sorption (absorption and adsorption) into metals and its relation to  $H$ -adsorption and surface poisoning effects were discussed by Jerkiewicz (1992) and Jerkiewicz and Conway (1992). Evidently, the operating driving force for sorption, which is the chemical potential gradient across the interphase region, must be clearly defined.

### 3.2.1 Chemical Potential of Absorbed Hydrogen

According to Wagner (1944), the chemical potential of dissolved hydrogen is given by

$$\mu = \mu^o + \left[ RT \ln\left(\frac{n}{I-n}\right) \right] + \Delta\mu \quad (1)$$

where  $n = H/Pd$  is the atomic ratio and  $\Delta\mu$  represents the deviation from the ideal distribution of  $H$  among the octahedral sites. In Wagner's formulation, the excess potential,  $\Delta\mu$ , is due to the contribution of hydrogen electrons. Later, Brodowsky (1972) added the protonic contribution so that

$$\Delta\mu = \Delta\mu_+ + \Delta\mu_- \quad (2)$$

resulting in the following picture to emerge:  $H$ -atoms within the octahedral positions are electronically screened protons with the screening charge occupying the broadened states in the  $4d$ -band and the delocalized states in the  $5s$ -band of the host lattice. While  $\Delta\mu_+$  is generated by vibrating protons,  $\Delta\mu_-$  is the electronic contribution, which increases sharply with an increase in  $H$ -atom concentration. In reality, the situation is further complicated by lattice expansion. Furthermore, changing the number of defects by generation of new defects arising from the lattice expansion, affects the chemical potential and through it, the transport into the bulk, the so-called Gorski effect (Voelkl, 1972).

### 3.2.2 Chemical Potential of Hydrogen in the Interphase

The chemical potential of molecules residing in the interphase region must reflect its non-autonomous character. Jerkiewicz and Conway (1992) treated the sites of adsorbed and absorbed  $H$  in terms of site fraction statistics in order to write down their chemical potentials. The efficiency of absorption, in relation to the hydrogen evolution reaction, can be examined in terms of the reaction mechanism. The effect of catalytic poisons promoting the absorption is discussed in terms of competition for the sites. The discussion focused on the complex nature of the interphase, however, it did not model the electrode response to the charging (discharging) currents. Within an electric field (i.e., the electric double layer) there is an increase in energy in the system which has not been included. Since the chemical potential of a molecule is affected by the electrode polarization, the picture presented by Jerkiewicz and Conway (1992) is incomplete and additional work is needed. In summary, the predictive capabilities of a model are determined by several factors, among them, the structure of the interphase and a full description of the operating driving force, including a complete expression for the gradient of the chemical potential, both in the bulk electrode and across the interphase.

## 4. TECHNOLOGY ISSUES

The development and construction of metal hydride electrodes for battery applications encompasses four areas of research: (i) the rate at which hydrogen can be recovered and brought into the reaction zone, (ii) the rate of charge transfer, (iii) the determination of the amount of hydrogen stored within the electrode structure, and (iv) reversibility. The first and second areas of research are concerned with the elementary processes and modeling while the third deals with the hydrogen sorption capacity. The fourth area of research deals with the degradation of the electrode upon cycling.

## 4.1 THEORETICAL ASPECTS

The cell/electrode modeling follows the rules first defined by Newman and Tobias (1962) and somewhat later extended to complex systems exhibiting unique features by, among others, Tsauro and Pollard (1984a, 1984b). A summary of the governing equations for the Tsauro–Pollard formulation for the *Li/SOCl<sub>2</sub>* system is given in Table I. With appropriate modifications, these equations can be adapted to represent the *MH*-system. The resultant modifications must reflect the characteristic features of the *MH*-electrode as displayed by experimental simulation. Furthermore, the need to include a synergistic interaction between the assumed events as shown from modeling and the behavior observed in experimental analogs cannot be overemphasized.

### 4.1.1 Review of *MH* Electrode Modeling

To date, only certain aspects of *MH* electrodes have been modeled. In general, these modeling approaches have treated the *MH* electrode as a planar surface in contact with an electrolyte separated by an interfacial region. For example, Luo et al. (Luo, Johnson, Feldberg, & Reilly, 1993) used a model based on diffusion out of a cylinder to describe the kinetics of discharge of the *Pd<sub>0.85</sub>Ni<sub>0.15</sub>* hydride electrode. In a separate exercise, Szpak et al. (Szpak, Gabriel, Smith, & Nowak, 1991) derived equations governing transport of *H* across the interphase into the bulk electrode for the *Pd/H<sub>2</sub>O* system and have obtained numerical solutions. In their model, they took into account the processes illustrated in Figure 1. This model assumed no geometrical restrictions on the electrolyte phase and agreed well with the experimental data obtained by Riley et al. (Riley, Seader, Pershing, & Walling, 1992) as was demonstrated by Szpak et al. (Szpak, Mosier–Boss, Gabriel, & Smith, 1994).

There has been some effort to place more realistic constraints upon the system when modeling. Recently Viitanen (1992,1993) has modeled the transport of *H* in a *MH* electrode comprised of spherical particles of uniform size. Mao and White (1991) modeled the self-discharge of a *NiOOH* electrode in a hydrogen environment. This model took into account diffusion of dissolved hydrogen in an electrolyte film which covers a flooded electrode, electrochemical oxidation of hydrogen, reduction of *NiOOH*, and changes in surface area and porosity of the electrode during the self-discharge process. Their model does not specifically pertain to the *MH* electrode; however, it does, peripherally, describe transport of an electrolyte phase in a porous structure.

### 4.1.2 Limitations of Current Models

Clearly, previous modeling of the *MH* system has been somewhat incomplete and limited to specific elements of the charging/discharging cycle. To our knowledge, no general model has been developed to describe the transport processes within and between the electrolyte and the hydrogen absorbing material during the course of cell/battery operation. Ideally, such a model would describe every aspect of *MH* charging/discharging. This is essential in order to predict the operational characteristics of the system, as a whole, and to assess the influence of changes in design parameters on the cell performance. Not only would such a model identify system limitations, but it would also help guide future experimental research.

As summarized in Table I, when modeling a charging/discharging cell, one must take into account the material balances, Faraday's law, Ohm's law, and the polarization equation. For the *MH*-electrode, we also have to include the energy balance, the effect of the interphase, and *H* transport between and within the particles making up the porous structure of the *MH* electrode. These latter effects will be taken into account by the form of the auxiliary equations. The development of a general model is a nontrivial undertaking since charging/discharging of a metal hydride is a very complicated process, as shown in Figure 1, and there are essentially three phases to consider—the electrolyte, the particles

DESCRIPTION	EQUATION
Material balances: (a) electrolyte species	$\frac{\partial(c c_i)}{\partial t} = a j_{in} - \nabla \cdot \underline{N}_i$
(b) solid phases	$\frac{\partial c}{\partial t} = \sum_{\text{solids}_i} \left( \sum_{\text{reactions}_k} \frac{s_{i,k} \tilde{V}_i}{n_k \mathcal{F}} (a i_n)_k - s_{i,o} \tilde{V}_i R_o \right)$
Flux relation for electrolyte species	$\underline{N}_i = -\epsilon D_{ie} \nabla c_e - \epsilon D_{ia} \nabla c_a + \frac{t_i^+ i_2}{z_i \mathcal{F}} + c_i v_i^*$
Faraday' law	$a j_{in} = - \sum_{\text{reactions}_k} \frac{s_{i,k}}{n_k \mathcal{F}} (a i_n)_k - s_{i,o} R_o$
Ohm's law, modified for electrolyte phase	$\frac{i_2}{\kappa} = \frac{(I - i_2)}{\sigma} + \nabla \eta - \frac{RT}{\mathcal{F}} \left\{ 2 \left( t_1^+ - 1 + \frac{c_e}{2c_o} \right) \nabla \ln c_e + \left( t_3^+ + \frac{c_a}{2c_o} \right) \nabla \ln c_a \right\}$
Polarization equation	$i_{nk} = i_{ok} \left[ \exp \left( \frac{\alpha_{ak} \mathcal{F} \eta_s}{RT} \right) - \exp \left( \frac{-\alpha_{ck} \mathcal{F} \eta_s}{RT} \right) \right]$
Equation to describe active specific surface area in cathode	$a = a^o \left[ 1 - \left( \frac{\epsilon_{LiCl}}{c_p} \right)^p \right]$
Equation to describe thickness of defective LiCl film at anode	$\frac{d\delta_f}{dt} = \tilde{V}_{LiCl} \left[ \frac{2D_f}{\delta_f} (c_o)_b - k_l (c_a)_b \right]$

**Table 1.** Summary of governing equations for  $Li/SOCl_2$  cells. (Adapted from Tsaur and Pollard, 1984a and 1984b). List of symbols and reaction equations for  $Li/SOCl_2$  electroreduction are found in sections 6.1 and 6.2, respectively.

making up the *MH* electrode, and bubble formation. Therefore, the appropriate equations would have to be formulated to include coupling of the electrode/electrolyte processes within this multiphase environment. From our viewpoint, previous modeling of the *MH* system suffers from a number of deficiencies. They are:

- (i) conservation of energy from which the temperature distribution is determined
- (ii) the interphase which is an active element in the transport of *H* and is non-autonomous (Ohnishi et al., 1993; Ciureanu et al., 1993; Dantzer, Pons, Guillot, & Cai, 1992; Cimato, Zhang, Goudy, & Singleton, 1992). A general model will have to include the effect of a changing interphase on *H* transport. The earlier model of the *Pd/H<sub>2</sub>O* system, by Szpak et al. (Szpak, Gabriel, Smith, & Nowak, 1991) partially treated this effect but will have to be extended.
- (iii) the effects of the electrode matrix and grain boundaries upon *H* transport. The electrode matrix refers to the porous electrode structure while the grain boundaries refer to the metallurgical aspects within individual particles. Consequently, we must deal with *H* transport between and within particles making up the porous structure. Transport within grain boundaries has been partially treated by Zaeschmar (1983). His formalism will require modification to be applicable for the *MH* electrode.

For the construction of the auxiliary equations, experimental data are needed regarding electrolyte transport properties and their dependence on temperature and composition, properties of the metal hydride as a function of loading (e.g., conductivities, densities, diffusion coefficient of *H*, etc.), kinetic parameters (e.g., exchange current densities, active specific surface areas, symmetry factors, and morphology parameters), etc. Although there are experimental discharge curves for working cells in the literature and a wealth of information on the kinetics of charge transfer for many half-cell reactions, pertinent input data on transport processes within porous structures are lacking.

Intuitively, one would expect interactive cooperation between modeling exercises and experiment since model construction and verification require that the calculated results match actual experimental data. Ideally such an interaction between modeling and experiment would be synergistic; experiments are designed and conducted to provide the data needed to aid in formulating the auxiliary equations in the model. Similarly, the model may predict a certain behavior which will have to be verified by experiment. Rarely does this synergistic interaction between modeling and experiment occur. Clearly, this is another area in modeling which is deficient. When the experimental data are not available. It is a common practice in modeling to employ the general Newman–Tobias formalism (Newman & Tobias, 1962) and simply vary the parameters in such a way that the results from the model, e.g., a calculated discharge curve, approximates that measured for a working cell. Dependent upon the number of parameters it is quite possible that a large number of solutions exist which would approximate the observed cell behavior.

## 4.2 SPECIFIC TASKS FOR MODELING

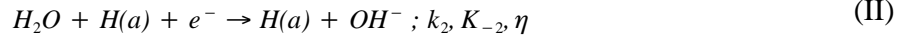
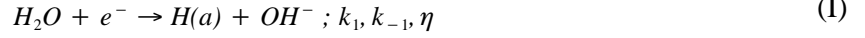
Developing a general model of the charging/discharging *MH* electrode would require (i) modification of the equations in Table I to describe transport processes within and between both the electrolyte and the hydrogen absorbing material; (ii) designing and building experimental analogs to secure such data as necessary for the construction and verification of the model; and (iii) examination of the factors affecting hydrogen sorption.

### 4.2.1 Development of Formalism for the *MH* Electrode

In developing a general model to describe the *MH*-electrode, we start with the concept that the processes occurring within a porous electrode correspond to those on a planar electrode subject to the

geometrical constraints imposed by the structure itself. A one dimensional model, consisting of compacted spheroid particles in contact with a current collector on one side and continuous electrolyte phase on the other, is assumed. Initially spherical particles of uniform size are considered. However, later modifications of the model would have to take into account particles of non-uniform size. The porous regions of the cell are assumed to be flooded.

The fluxes involved in charging the metal hydride electrochemically are summarized in Figure 1. When charging the *MH* electrode, reduction of water must first occur, via the Volmer path, Equation (I), or the Heyrovsky–Horiuti path, Equation (II),



with gas evolution occurring by the Tafel path, Equation (III),



Here (*a*) and (*s*) denote species present in an adsorbed state and in solution, respectively. The absorption into the lattice of electrochemically generated hydrogen is given by Equation (IV)



where (*l*) denotes the species in the lattice.

For discharge, the reactions taking place at the surface of the metal particles are the reverse of reactions (IV) and (I). The reverse of reaction (IV) is the dehydridization reaction, where the hydrogen is released from the hydride phase, resulting in the formation of adsorbed hydrogen atoms. The electrochemical reaction, in which current is generated when the adsorbed hydrogen reacts with hydroxide ions, is the reverse of reaction (I). Gas evolution occurs via the Tafel path, Equation (III).

Returning to the summary of equations presented in Table I, the material balance equation for the electrolyte species requires no further modification for the *MH* system. However, the solid phase material balance equation will have to be modified to take into account the change in volume of the particles during charging/discharging and grain size boundaries. During charging/discharging, the metal hydride particles expand/contract resulting in porosity changes. The upper and lower limits would be the total volume of particles fully loaded with hydrogen and virgin material which has not undergone a charge/discharge cycle, respectively. Once a hydrogen absorbing material has undergone a charging cycle, the lattice does not collapse back to its pre-loaded condition. The degree of expansion/contraction of the particles making up the *MH* electrode is a function of the degree of loading. Modifying the solid phase material balance to take into account grain boundaries is more difficult. Grain boundaries represent locations of a high density of lattice imperfections. The major effect grain boundaries have on charging/discharging is on the diffusion of hydrogen into the lattice. The interaction of an interstitial with a lattice defect is energetically quite different from its interaction with the undisturbed lattice. One approach is to treat grain boundaries as internal surfaces on the spherical *MH* particles where an exchange process similar to adsorption-desorption can occur.

Although the flux relation equation for the electrolyte species in Table I can be used for the *MH* electrode without further modification, simplifications may result from the introduction of effective parameters, e.g.,  $D_{eff}$ . However, a corresponding flux relation equation will have to be derived for diffusion of hydrogen into the solid state particles. This latter equation will be dependent upon the surface coverage of adsorbed hydrogen atoms.

The expression for Faraday's law in Table I is applicable to the *MH* electrode. However, the expression for Ohm's law will have to be reformulated to comply with the *MH* system. The polarization equation in Table I will also have to be extended to include changes in the reaction path resulting from the influence of an active interphase. The auxiliary equation in Table I which describes the thickness of the defective *LiCl* film at the anode is not applicable to the *MH* system and will be excluded. Conversely, the auxiliary equation, which describes the active specific surface area in the cathode, will be modified for the *MH* electrode. In particular, the specific surface area,  $\alpha$ , is a function of  $\varepsilon$ ,  $c_i$ , and  $j$ . This latter equation will also have to include the effect of gas evolution since gas bubbles will effectively block the active sites on the particles.

An additional equation is required to take into account the energy balance. A comprehensive treatment of thermal effects in electrochemical cells is given by, among others, Newman (1973). As a starting point, the temperature distribution is obtained by assuming a conservation of energy. The state of any system is completely characterized by the internal energy,  $U$ ; the volume,  $V$ ; and the mole number,  $n_j$ . For systems under constant pressure, the use of the enthalpy function is more convenient. The transition from energy to enthalpy representation is made by substituting volume with pressure so that  $H^{(\alpha)} = H^{(\alpha)}(T, P, n_j)$ .

Identifying the porous structure as an open system and applying energy conservation in the enthalpy representation to a subsystem,  $\alpha$ , the change in the enthalpy is given by

$$\frac{\partial H^{(\alpha)}}{\partial T} \Big|_{n_j} dT + \frac{\partial H^{(\alpha)}}{\partial n_j} \Big|_T dn_j = dq^{(\alpha)} - dw^{(\alpha)} + dq^{(\alpha \rightarrow \beta)} \quad (3)$$

where  $\alpha$  and  $\beta$  designate subsystems in contact with each other. In equation (3),  $dq$  is the heat of reaction (e.g., absorption),  $dw$  is the work done by the system (e.g., electrical work), and  $dq^{(\alpha \rightarrow \beta)}$  is the heat transferred from subsystem  $\alpha$  to subsystem  $\beta$ . The temperature distribution,  $T(x, t)$ , is calculated from the change in the enthalpy  $H^{(\alpha)}$  occurring within time,  $dt$ , viz.,

$$C_p^\alpha \frac{dT^\alpha}{dt} = dJ_q^{(\alpha)} - dJ_q^{(\alpha \rightarrow \beta)} \quad (4)$$

where  $\alpha$  denotes the position in coordinate  $x$ . By identifying subsystem  $\alpha$  with position, we identify a continuous system, as shown in Figure 2. A complete treatment, including mass and momentum balance, leading to the temperature distribution is given in, e.g., Haase (1969).

The effect of an active, non-autonomous interphase will be taken into account by an auxiliary equation. Inclusion of diffusional transport of hydrogen into the lattice through an active interphase necessitates the separation of the interphase region from the diffusional space. In their model of charging of the *Pd* lattice, Szpak et al. (Szpak, Gabriel, Smith, & Nowak, 1991) treated the bulk electrode as a body consisting of  $N$  layers; the  $i^{th}$  layer having a volume  $V_i$  and the area of the dividing surface between it and the  $(i + 1)^{th}$  is  $S_{i,i+1}$ . In general,  $V_i \neq V_{i+1}$  and  $S_{i-1,i} \neq S_{i,i+1}$ . The diffusion of hydrogen in the bulk of the solid body was considered to be the process of jumping from one layer to an adjacent layer with a rate that is proportional to the interfacial area between the layers, as well as the number of vacant sites in the final layer. The boundary conditions are determined by the physical considerations of events occurring at the 1<sup>st</sup> and  $N^{th}$  layers. This treatment will have to be extended to an interphase which actively participates in hydrogen transport into the lattice and whose structure changes throughout the charging/discharging cycle. As the loading increases/decreases during charging/discharging, the number and thicknesses of the layers,  $N$ , making up the interphase vary as does the number of available sites within a layer and the jump rate constant between layers.

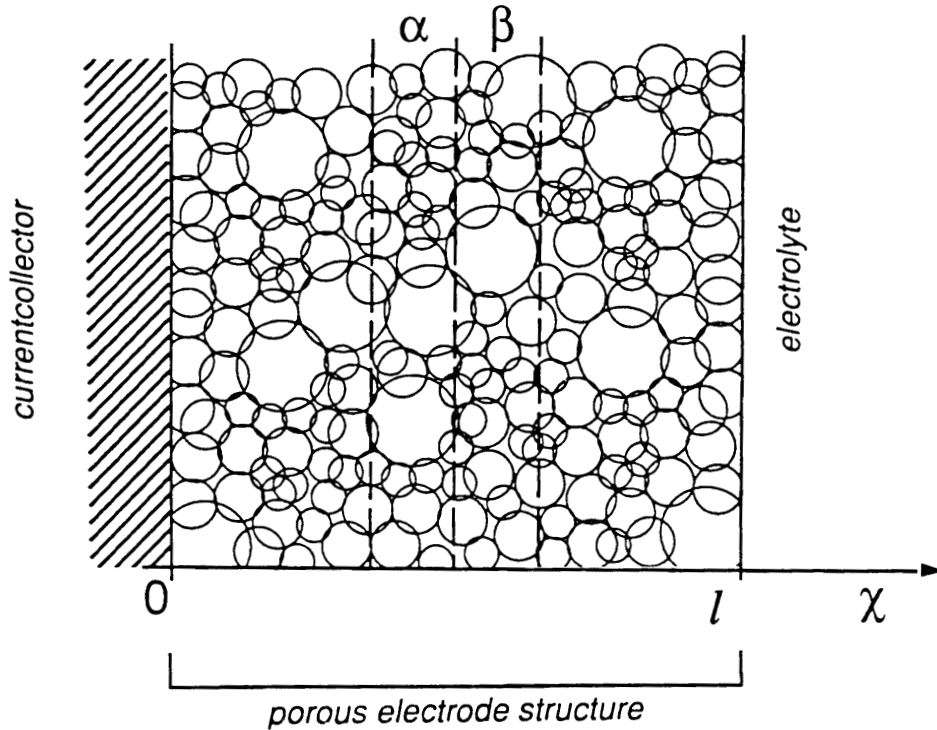


**Figure 2.** One-dimensional model of a porous structure showing  $\alpha$ ,  $\beta$  subsystems.

#### 4.3 EXPERIMENTAL ASPECTS: MODEL CONSTRUCTION AND VERIFICATION

The exact form of the expressions used to describe the *MH* electrode during charging/discharging will be dependent upon the measured response of experimental analogs. These experimental analogs are used to simulate the behavior of a working cell, thereby providing the input data required for construction and verification of the model. The input data needed for model construction/verification are:

- (i) electrolyte transport properties and their dependence on temperature and composition
- (ii) solid phase conductivities and densities
- (iii) metallurgical aspects of the *MH* electrode as a function of loading
- (iv) the open-circuit cell potential and its dependence on temperature
- (v) hydrogen absorption capacities and rates of charging/discharging
- (vi) kinetic parameters: e.g., exchange current densities, active specific surface areas, symmetry factors, morphology parameters, and effects of the interphase

With this information at hand, the model can be used to predict the time and position-dependent behavior of the system.

##### 4.3.1 Simulations

For realistic representation, the proposed model must be based on analyses of the actual elementary processes occurring within the confines of the porous structure. Experimental data on local and bulk transport and charge transfer kinetics are needed. Similarly, data are needed on the variation in the

driving force which occurs naturally as a function of distance as well as morphological changes for any given mode of operation. Such data are difficult to obtain in-situ since the insertion of probes compromises the integrity of the porous structure. Instead we propose to use simpler experimental arrangements that are designed to simulate the behavior of practical electrodes. The intent of simulation is to represent the real system by one which is accessible to direct observation so that the effects of varying structural electrochemical, and transport phenomena can be followed using ultramicroelectrodes and optical techniques. In the simulation attempt, we select a configuration that exhibits some or all of the features common to the operating system. An example of the evolution of an experimental analog to represent a single-pore is illustrated in Figure 3.

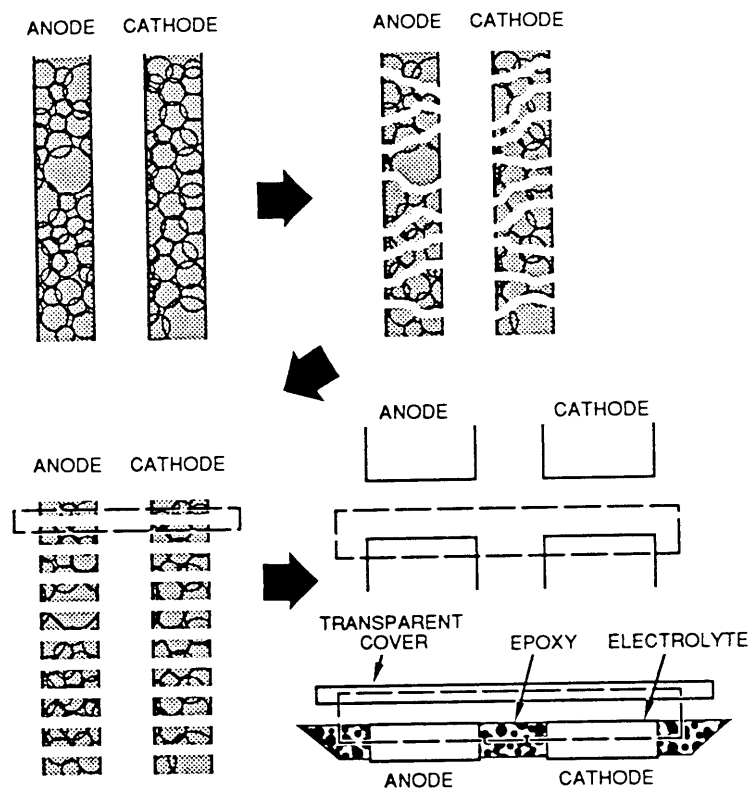


**Figure 3.** Schematic derivation of single-pore analog cell through successive degrees of abstraction: A real electrode consisting of interconnected pores and bonded particles; B, idealized abstraction of A, retaining tortuous pores, but pores are no longer interconnected; C, further abstraction where pores pass straight through the electrodes (tortuosity factor = 1); D, section through the cell, shown as an abstraction and as the analog single-pore cell.

Since we are interested in obtaining data on transport processes within a porous structure, we would use a segmented electrode similar to that shown in Figure 4 as an experimental tool. This particular experimental design was used to study the current density,  $j(x, t)$ , dependence of the  $Ag/AgCl$  system (Szpak & Katan, 1975; Szpak, Nedoluha, & Katan, 1975). In the construction of the experimental analog, a silver working electrode consisting of several segments as shown in Figure 3, is vapor deposited onto a glass microscope slide. The layer of silver will act as a current collector and a substrate onto which a hydrogen sorbing material will be deposited. The silver has the added advantage of acting as a barrier to diffusion of sorbed hydrogen within the absorbate. Since there is a wealth of data available for electrochemical loading/unloading of  $Pd/H$ , this system is often employed as a model. In addition, some commercially available  $MH$  materials for battery applications are coated

with a catalytic surface of *Pd*. Therefore, initially, the hydrogen sorbing material would consist of *Pd*, either vapor or electrochemically deposited onto the *Ag* substrate. Later commercially available *AB*<sub>2</sub> and *AB*<sub>5</sub> materials would be employed once the experimental details have been established. These materials are particulate and will have to be mixed with *Ag* to provide a conductive path, sintered, and connected to the segmented *Ag* current collector on the glass slide. In order to make direct measurements of the space-time distributions of transfer current,  $j(x, t)$ , the thin segments of the electrode structure must be isolated and provided with a separate current take off lead. This should be done so that the sectioning will not appreciably change the structure and elementary processes that comprise the over-all reaction path. Also provisions must be made to assure the monitoring of current in each segment without altering the original  $j(x, t)$  distribution.

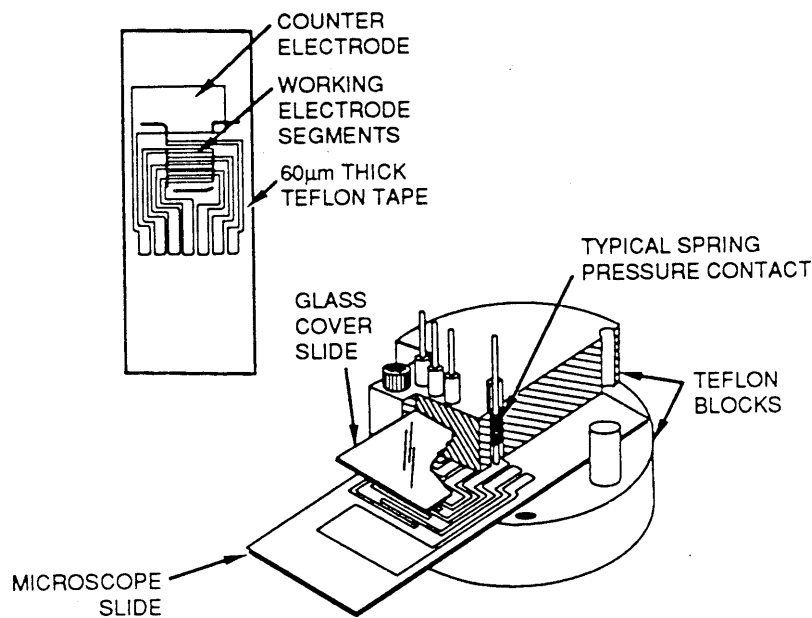


**Figure 4.** Experimental cell assembly. Lower right: details of holder construction, electrical connections, and positioning of segmented electrode. Upper left: construction of segmented electrode showing vapor deposited silver on a glass substrate. The shaded area is a U-shaped Teflon tape, 60  $\mu\text{m}$  thick.

The experimental cell assembly, illustrated in Figure 4, lends itself to additional measurements besides that of  $j(x, t)$ . These include both electrochemical as well as optical measurements. For example, the rate of *H* absorption/desorption can be studied under both potentiostatic and galvanostatic conditions. The working electrode can be pulsed either potentiostatically or galvanostatically while the behavior of the segments making up the working electrode are monitored individually. These techniques are often used to probe the kinetics of mass transport, charge transfer, coupled chemical reaction rates, and absorption (Bard & Faulkner, 1980; R.W. Murray, 1986). In addition, AC impedance spectra can be recorded while the electrode is pulsed either potentiostatically or galvanostatically. These spectra are examined in terms of by an equivalent electric circuit analog, thus indicating which process(es) controls the electrode behavior (MacDonald, 1987). Conway (1965) has represented electrode processes using such analogs. However, these circuits are not complete for the hydrogen absorbing electrodes because the processes occurring in the solid phase are not included.

Also the cell assembly, shown in Figure 4, can provide information on the evolution of the temperature profile,  $T(x, t)$ , and the concentration gradients,  $\nabla c(x, t)$ . To measure  $T(x, t)$ , small differences in temperature can be displayed by simply replacing the glass cover by a plastic sheet impregnated with

a liquid crystal (Driscoll & Szpak, 1985). The concentration gradients in the electrolyte phase can be viewed with the aid of a Watson interference objective. Using such an apparatus, one can monitor, in real time, local changes in the electrolyte phase. An example, shown in Figure 5, demonstrates the

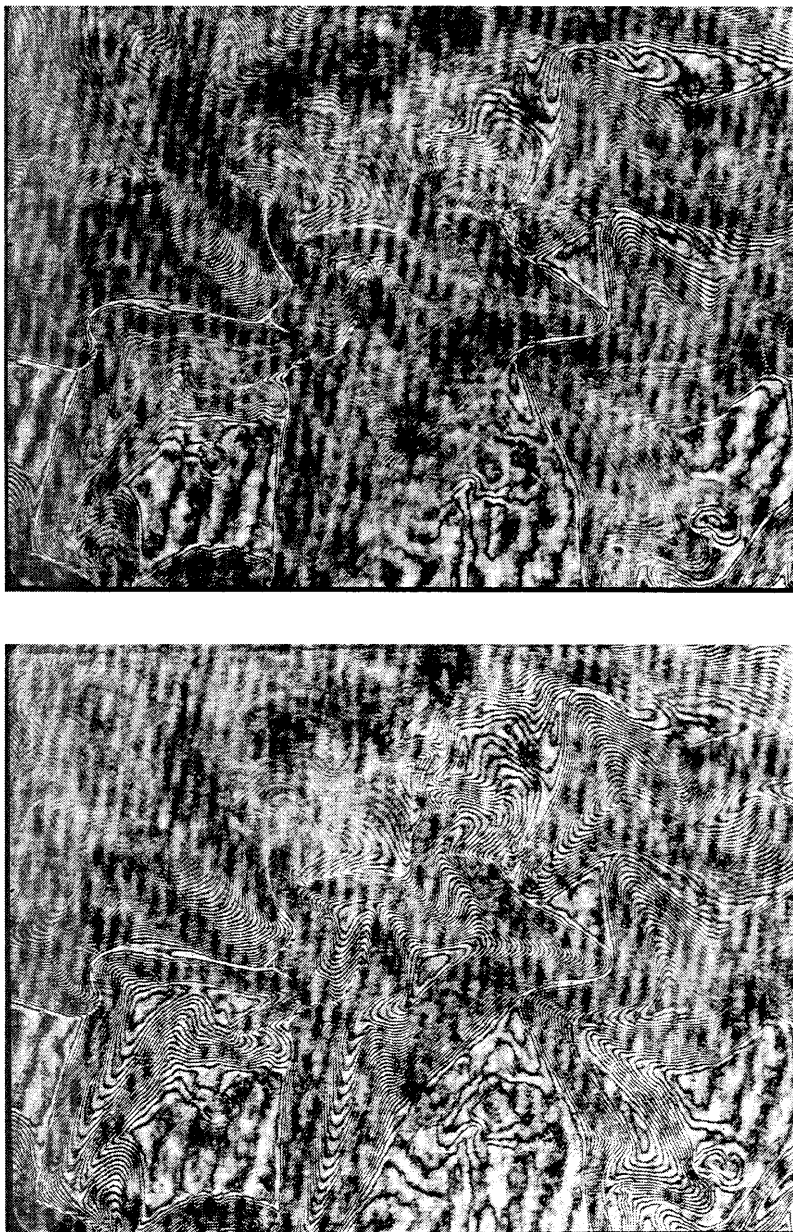


**Figure 5.** Development of concentration gradients in an experimental cell, similar to that shown in Figure 4, as displayed with the aid of a Watson interference objective. Electrode reaction:  $Zn \rightarrow Zn^{+2} + 2e^{-}$ ; galvanostatic conditions  $j = 10 \text{ mA cm}^{-2}$ ; distance  $x = 0.3 \text{ cm}$ ; the time between exposures is 60 s.

localized nature of the charge transfer reaction and resultant concentration gradients as well as their movement with the passage of time. These observations, when examined against the structural features of the porous electrode, may lead to the rational specification of the “effective parameter,” i.e., in the dependence between process coupling and the geometrical features of the electrode interior.

### 4.3.2 Examination of the Electrode/Electrolyte Interphase

The properties of the electrode/electrolyte interphase are governed by solution and electrode composition as well as the metallurgy of the electrode, e.g., grain size, grain boundaries, and the density of defects. During charging/discharging, changes in the structure and appearance of the electrode surface occur and reflect the contributions of an active electrode/electrolyte interphase. For example, Rolison et al. (Rolison, O’Grady, Doyle, & Trzaskoma, 1990) demonstrated for *Pd* electrodes, during prolonged exposure to hydrogen and deuterium, that the active participation of the surface manifested itself as inhomogenous changes in the surface morphology. A realistic model must, therefore, include an active, changing electrode/electrolyte interphase. This is very difficult to accomplish since there are limited realtime, in-situ data on the morphological changes of the electrode surface during charging and/or discharging. Most of the data that is available is from ex-situ post-test examination of electrodes which have undergone several charging/discharging cycles. Experiments must be designed which will provide the necessary data to aid in developing the model.

**4.3.2.1 Relevant Experimental Tools.** One way to demonstrate the inhomogeneity of a surface, particularly with regard to absorption, is to view it using nomarski optics (Szpak, Mosier-Boss, Gabriel, & Smith, 1994) so that regions of preferred absorption can be differentiated. An example of an experimental arrangement is illustrated in figure 6. This arrangement allows continuous in-situ monitoring of the electrode surface during charging/discharging. The usefulness of this technique to monitor changes in the *Pd/H<sub>2</sub>O* interphase during the uptake of electrochemically generated hydrogen has been demonstrated (Szpak, Mosier-Boss, Gabriel, & Smith, 1994).

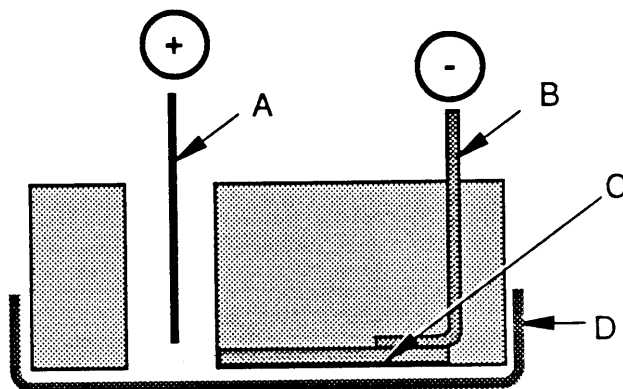


**Figure 6.** Electrolytic cell for the examination of an electrode surface by Nomarski optics. A = *Pt* counter electrode; B = *Cu* wire spotwelded to *Pd* electrode; C = etched *Pd* surface; D = Mylar film.

Since the properties of the interphase are determined by those of the contacting phases, i.e., the electrode interior as well as the electrolyte, the extent to which the electrode/electrolyte interphase facilitates hydrogen sorption can be modified by changing the composition of either phase. One modification of interest is the introduction of surface active impurities and their effect on the performance characteristics. Examples of additives which strongly modify the behavior of the *Pd/H<sub>2</sub>O* system are thiourea,  $Al_2O_3$ , and cyanide ion. The effect of these and other additives on hydrogen sorption of the

$AB_2$  and  $AB_5$  alloys must be ascertained via cyclic voltammetry, galvanostatic and potentiostatic pulsing, and AC impedance techniques. The results of these studies will provide a greater understanding on how the interphase influences hydrogen sorption and will facilitate development of the auxiliary equations in the model.

### 4.3.3 Experimental Cell to Monitor Hydrogen Sorption

Practical electrodes consist of particles of the hydrogen-absorbing material embedded in a conductive matrix, such as foamed *Ni*. Data on the hydrogen absorption capacity and rates of charging/discharging of the material need to be known for complete modeling. Such data are also needed in order to determine which material is best for a given application and to optimize the composition of that material to meet the performance criteria. These quantities for the  $AB_2$  and  $AB_5$  materials should be measured as a function of electrode and electrolyte composition.

The amount of hydrogen stored within the electrode structure and the rate at which it can be transferred across the interphase in both directions can be monitored using a cell similar in design as that described by Will et al. (1991). This cell, in modified form, is illustrated in Figure 7. In this sealed

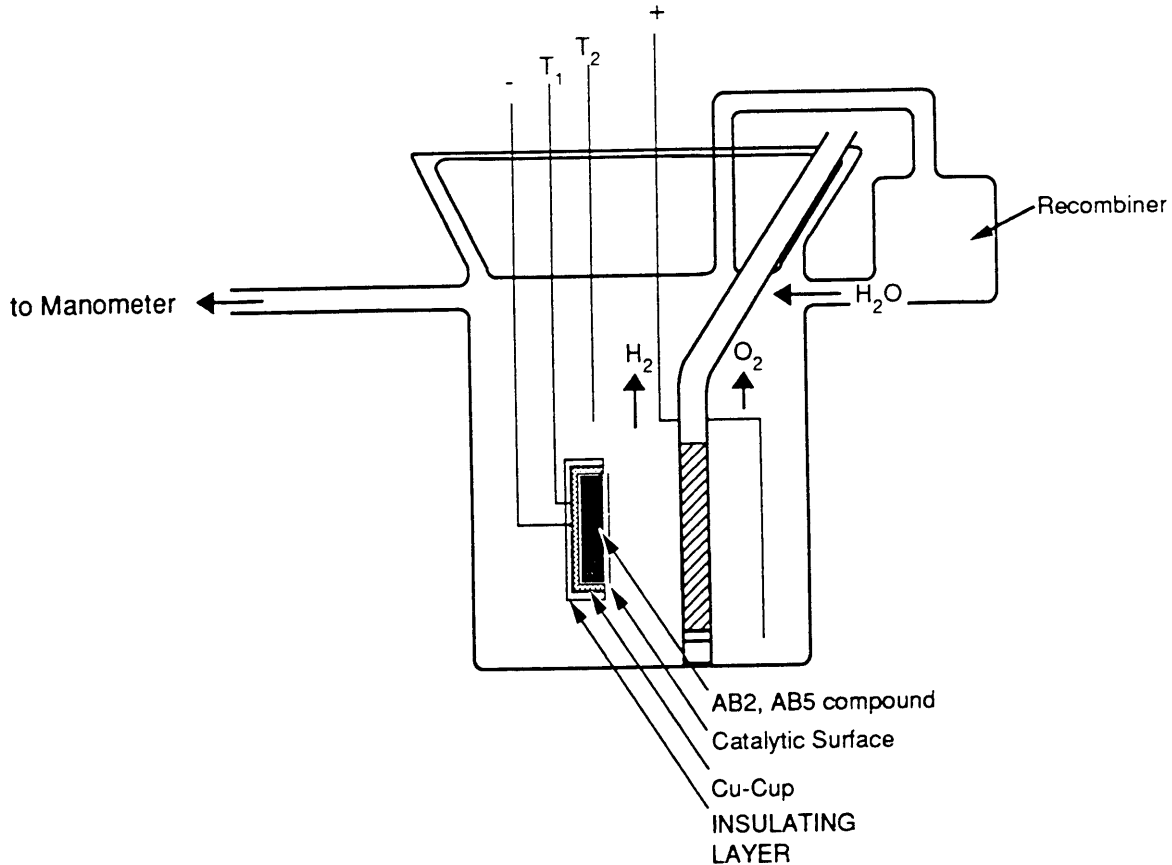


**Figure 7.** Design of the experimental cell.  $T_1$  and  $T_2$  refer to the temperatures of the *MH* electrode and solution, respectively.

cell, the *MH* working electrode is separated from the counter electrode by a fritted glass plate to prevent direct contact between  $O_2$  gas and  $H_2$  gas generated during charging of the catalytic walls of the *MH* electrode. After cell assembly, the space above the electrolyte is filled with  $H_2$  and the pressure is recorded. During electrolysis (charging),  $H_2$  gas generated at the *MH* electrode either transports into

the solid or transfers into the gas phase. The gaseous  $O_2$  generated at the positive electrode enters the gas phase above the anolyte and is recombined on the surface of a  $Pt$  catalyst. The amount of absorbed hydrogen and the rate at which absorption has occurred is calculated from the pressure changes in the gas phase. To equalize the liquid level and the pressure in both compartments, shunting is provided.

## 5. CONCLUDING REMARKS

The relevance of modeling to the development of metal hydride technology can be summarized as follows:

1. Theoretical modeling deals with problems of general/broad applicability, i.e., it assumes a physical model (arrangement) and provides solutions for mathematical statements (equations). The connection with reality is thus limited by the input parameters, the values of which are often unknown.
2. To be effective as a development guide, parameters relevant to the selected system must be obtained. These parameters, in turn, determine the performance envelope.
3. In real electrode systems, mathematical formulation may be so complex that unambiguous interpretation is not possible. In such cases, experimental simulation may be helpful in displaying the most important features, thereby, reducing computation and providing a more realistic guidance.

## 6. SYMBOLS AND CHEMICAL EQUATIONS USED TO DERIVE EXPRESSIONS IN TABLE I

### 6.1 LIST OF SYMBOLS USED IN EQUATIONS IN TABLE I

$\alpha$	interfacial area per unit volume ( $\text{cm}^{-1}$ )
$c_a$	molar concentration of $AlCl_3$ (mole $\text{cm}^{-3}$ )
$c_e$	molar concentration of electrolyte (mole $\text{cm}^{-3}$ )
$c_i$	molar concentration of species $i$ (mole $\text{cm}^{-3}$ )
$c_e^o$	initial electrolyte concentration (mole $\text{cm}^{-3}$ )
$c_o$	molar concentration of solvent (mole $\text{cm}^{-3}$ )
$D_f$	effective diffusivity of $SOCl_2$ in $LiCl$ film ( $\text{cm}^2 \text{s}^{-1}$ )
$D_{ia}$	diffusion coefficient for acid ( $\text{cm}^2 \text{s}^{-1}$ )
$D_{ie}$	diffusion coefficient for electrolyte ( $\text{cm}^2 \text{s}^{-1}$ )
$\mathcal{F}$	Faraday's constant (96,487 C/equiv)
$i_{ok}$	exchange current density for reaction $k$ ( $\text{A cm}^{-2}$ )
$i_2$	superficial current density in pore phase ( $\text{A cm}^{-2}$ )

$i_{nk}$	local current density due to reaction k (A cm <sup>-2</sup> @)
$I$	superficial current density to an electrode (A cm <sup>-2</sup> @)
$j_{in}$	pore wall flux of species i (mole cm <sup>-2</sup> s <sup>-1</sup> )
$k_l$	rate constant of reaction (III) at anode (cm s <sup>-1</sup> )
$L$	electrode thickness (cm)
$n_k$	number of electrons transferred in electrode reaction k
$\underline{N}_i$	superficial flux of species i (mole cm <sup>-2</sup> s <sup>-1</sup> )
$p$	morphology parameter
$R$	universal gas constant (8.3142 J mole <sup>-1</sup> K <sup>-1</sup> )
$R_0$	reaction rate of chemical reaction (III) at cathode (mole cm <sup>-3</sup> s <sup>-1</sup> )
$s_{i,o}$	stoichiometric coefficient of species i in chemical reaction
$s_{i,k}$	stoichiometric coefficient of species i in electrode reaction k
$t$	time (s)
$t_i^*$	transference number of species i with respect to the volume average velocity
$T$	absolute temperature (K)
$\tilde{V}_i$	molar volume of species i (mole cm <sup>-3</sup> )
$z_i$	valence or charge number of species i
$\alpha_a$	transfer coefficient in anodic direction
$\alpha_c$	transfer coefficient in cathodic direction
$\delta_{LiCl}$	<i>LiCl</i> film thickness (cm)
$\varepsilon$	porosity or void volume fraction
$\varepsilon_{LiCl}$	volume fraction of <i>LiCl</i>
$\eta$	$= \phi_1 - \phi_2$
$\eta_s$	surface overpotential (V)
$\kappa$	effective solution conductivity (mho cm <sup>-1</sup> )
$\sigma$	effective matrix conductivity (mho cm <sup>-1</sup> )
$\phi_1$	electric potential in electrode matrix (V)
$\phi_2$	electric potential in the solution (V)

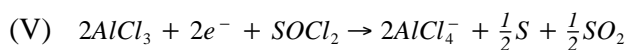
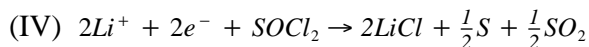
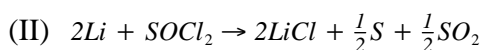
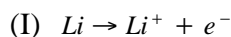
*Subscripts :*

<i>a</i>	$AlCl_3$
<i>b</i>	$LiCl$ film/separator interface
<i>e</i>	electrolyte
<i>f</i>	$LiCl$ film
<i>k</i>	reaction $k$
<i>p</i>	positive electrode
<i>s</i>	separator

*Superscript:*

<i>o</i>	initial
----------	---------

## 6.2 REACTIONS CONSIDERED IN DERIVING EQUATIONS IN TABLE I



## 7. REFERENCES

- Bard, A. J. and L. R. Faulkner. 1980. *Electrochemical Methods: Fundamentals and Applications*, John Wiley and Sons, Inc., New York, NY.
- Brodowsky, H. 1972. "Nomideal Solution Behavior of Hydrogen in Metals," *Ber. Bunsenges. Phys. Chem.*, 76, 740.
- Canet, O., M. Latroche, A. Percheron-Guegan, J. C. Archard, J. Bouet, and B. Pichon. 1992. "Characterization of New Laves Phases Hydrides for Electrochemical Applications," *International Symposium on Metal-Hydrogen Systems*. Uppsala, Sweden.
- Cimato, J., W. Zhang, A. J. Goudy, and K. R. Singleton. 1992. "The Hydriding and Dehydriding Kinetics of Some  $AB_5$ -type Hydrogen Storage Alloys," *International Symposium on Metal-Hydrogen Systems*, Uppsala, Sweden.
- Ciureanu, M., J. O. Strom-Olsen, D. H. Ryan, P. Rudkowski, and G. Rudkowska. 1993. "Rechargeable Batteries with Amorphous NiZr Hydride Electrodes," *184th Electrochemical Society Meeting*, New Orleans, Louisiana.
- Conway, B. E. 1965. *Theory and Principles of Electrode Processes*, The Ronald Press Co., New York, NY.

- Dantzer, P., M. Pons, A. Guillot, and H. Y. Cai. 1992. "Hydriding Kinetics in Intermetallic  $AB_5$  Hydrogen Storage Alloys," *International Symposium on Metal-Hydrogen Systems*, Uppsala, Sweden.
- Desilvestro, J., P. Reymond, J. Larcin, and P. Ruetschi. 1993. "Nickel Metal Hydride Batteries: From Button Cells to 50 Ah Batteries," *184th Electrochemical Society Meeting*, New Orleans, Louisiana.
- Driscoll, J. R. and S. Szpak. 1985. "Thermal Behavior of Electrochemical Cells by Liquid Crystal Display," *J. Power Sources*, 14, 321.
- Florino, M. E., K. Konstadinis, R. Opila, and C. W. Fang. 1993. "Surface Composition of a Misch-Metal Based  $AB_5$  Compound," *184th Electrochemical Society Meeting*, New Orleans, Louisiana.
- Friedrich, B. 1992. "Electrode Materials," *International Symposium on Metal-Hydrogen Systems*, Uppsala, Sweden.
- Haase, R. 1969. *Thermodynamics of Irreversible Processes*, Chapter 4, Addison-Wesley Publishing Co., Reading-Menlo Park-London-Ontario.
- Hasegawa, K., M. Oshnishi, M. Oshitani, T. Takeshima, Y. Matsumaru, and K. Tamura. 1992. "Nickel-Metal Hydride Battery," *International Symposium on Metal-Hydrogen Systems*, Uppsala, Sweden.
- Ise, T., K. Moriwaki, K. Nishio, M. Nogami, N. Inoue, M. Kimoto, M. Tadokoro, and N. Furukawa. 1992. "Development of  $H$ -Absorbing Alloys for  $Ni - MH$  Secondary Batteries," *International Symposium on Metal-Hydrogen Systems*, Uppsala, Sweden.
- Jerkiewicz, G. 1992. "Electrochemical and Chemical Aspects of  $Me-H$  Systems," *International Symposium on Metal-Hydrogen Systems*, Uppsala, Sweden.
- Jerkiewicz, G. and B. E. Conway. 1992. "Thermodynamics and Electrode-Kinetic Factors in Cathodic  $H$ -sorption into Metals and its relation to  $H$  Adsorption and Surface Poisoning Effects," *International Symposium on Metal-Hydrogen Systems*, Uppsala, Sweden.
- Kanda, M., S. Tsuruta, Y. Hanakata, H. Hasebe, and M. Yamamoto. 1992. "An Impedance Study on  $MmNi_5$  Type Metal Hydride Electrodes," *International Symposium on Metal-Hydrogen Systems*, Uppsala, Sweden.
- Kuriyama, N., T. Sakai, H. Miyamura, I. Uehara, and H. Ishikawa. 1992. "Deterioration Mechanism of  $MH$  Electrodes," *International Symposium on Metal-Hydrogen Systems*, Uppsala, Sweden.
- Luo, W., J. R. Johnson, S. W. Feldberg, and J. J. Reilly. 1993. "Properties and Discharge Kinetics of a  $Pd$  Activated  $Pd_{0.85}Ni_{0.15}$  Hydride Electrode," *184th Electrochemical Society Meeting*, New Orleans, Louisiana.
- MacDonald, J. R.. 1987. *Impedance Spectroscopy*, John Wiley and Sons, Inc., New York, NY.
- Mao, Z. and R. E. White. 1991. "A Mathematical Model of the Self-Discharge of a  $Ni - H_2$  Battery," *J. Electrochem. Soc.*, 138, 3354.
- Murray, R. W. 1986. "Chronoamperometry, Chronocoulometry, and Chronopotentiometry," in *Physical Methods of Chemistry Volume II: Electrochemical Methods*, John Wiley and Sons, Inc. New York, NY.

- Newman, J. and C. W. Tobias. 1962. "Theoretical Analysis of Current Distribution in Porous Electrodes," *J. Electrochem. Soc.*, 109,1183.
- Newman, J. 1973. *Electrochemical Systems*, Chapter 13, Prentice Hall, Inc., Englewood Cliffs, N.J.
- Ohnishi, M., Y. Matsumura, M. Kuzuhara, M. Watada, and M. Oshitani. 1993. "A High Energy Density Ni – MH Battery Using a Pasted Type Nickel Electrode and a MmNiAlCo Alloy Electrode," *184th Electrochemical Society Meeting*, New Orleans, Louisiana.
- Riley, A. M., J. D. Seader, D. W. Pershing, and C. Walling. 1992. "An In-Situ Method for Dynamically Measuring the Absorption of Deuterium in Palladium During Electrolysis," *J. Electrochem. Soc.*, 139,1342.
- Rolison, D., W. E. O'Grady, R. J. Doyle, Jr., and P. P. Trzaskoma. 1990. "Anomalies in the Surface Analysis of Deuterated Palladium," *The First Annual Conference on Cold Fusion*, Salt Lake City, UT.
- Stauffer, L., H. Ezzehar, and H. Dreyse. 1992. "Stability of Hydrogen Clusters Near a Transition Metal Surface," *International Symposium On Metal-Hydrogen Systems*, Uppsala, Sweden.
- Suda, S. and G. Sandrock. 1992. "Three Decades of Intermetallic Hydrides: What Happened to the Applications?," *International Symposium on Metal-Hydrogen Systems*, Uppsala, Sweden.
- Szpak, S., A. Nedoluha, and T. Katan. 1975. "Silver/Silver Chloride Electrode: Charging of a Porous Structure," *J. Electrochem. Soc.*, 122, 1055.
- Szpak, S. and T. Katan. 1975. "An Experimental Study of Reaction Profiles in Porous Electrodes," *J. Electrochem. Soc.*, 122,1063.
- Szpak, S. and J. J. Smith. 1990. "Transition Issues Associated with the Development of the Li/SOCl<sub>2</sub> Battery Technology", *Naval Research Reviews*, Vol. XLII, 12.
- Szpak, S., C. J. Gabriel, J. J. Smith, and R. J. Nowak. 1991. "Electrochemical Charging of Pd Rods," *J. Electroanal. Chem.*, 309, 273.
- Szpak, S., P. A. Mosier-Boss, S.R. Scharber, and J.J. Smith. 1992. "Charging of the Pd<sup>n</sup>H System: Role of the Interphase," *J. Electroanal. Chem.*, 337, 147.
- Szpak, S., P. A. Mosier-Boss, C. J. Gabriel, and J. J. Smith. 1994. "Absorption of Deuterium in Palladium Rods: Model vs. Experiment," *J. Electroanal. Chem.*, in press.
- Tsaur, K. C. and R. Pollard. 1984a. "Mathematical Modeling of the Lithium, Thionyl Chloride Static Cell. I. Neutral Electrolyte," *J. Electrochem. Soc.*, 131, 975.
- Tsaur, K. C. and R. Pollard. 1984b. "Mathematical Modeling of the Lithium, Thionyl Chloride Static Cell. II. Acid Electrolyte," *J. Electrochem. Soc.*, 131, 984.
- Uchito, H. and S. Hashimoto. 1992. "Effect of Surface Contamination on the Hydride of LaNi<sub>4.5</sub>Al<sub>0.5</sub>," *International Symposium on MetalHydrogen Systems*, Uppsala, Sweden.
- U.S. Department of Energy, Division of Chemical Sciences, Office of Basic Energy Sciences. 1992. Argonne National Laboratory. *Workshop on Advanced Battery Technology Research and Development*, Argonne National Laboratory.

- Viitanen, M. 1992. "A Mathematical Model for Metal Hydride Electrode," *NASA Technical Report PB92-136696*.
- Viitanen, M. 1993. "A Mathematical Model for Metal Hydride Electrodes," *J. Electrochem. Soc.*, 140. 936.
- Voelkl, J., 1972. "Gorsky Effect," *Ber. Bunsenges. Phys. Chem.*, 76, 797.
- Wagner, C. 1944. "Zur Deutung der Hystereseeerscheinungen in System PalladiumWasserstoff sowie bei Rotationsumwandlungen," *Z. Phys. Chemie. A*193, 386.
- Will, F. G., K. Cedzyska, M-C Yang, J. R. Peterson, H. E. Bergeson, S. C. Barrowes, W. J. West, and D. C. Linton. 1991. "Studies of Electrolytic and Gas Phase Loading of Palladium With Deuterium," *The Science of Cold Fusion: Proceedings of the Second Annual Conference on Cold Fusion*, Como, Italy.
- Yunshi, Z., C. Youviao, C. Jun, W. Da, and Y. Huatang. 1992. "Metal Hydride Electrode for Sealed Ni - MH Battery," *International Symposium on Metal-Hydrogen Systems*, Uppsala, Sweden.
- Zaeschmar, G. 1983. "Theory of Diffusion in Polycrystalline Materials," *J. of App. Physics*, 54, 2281.
- Zeuttel, A. 1992. "Effect of Partial Substitution of Ni in AB<sub>2</sub>-type Zr - Ni Alloys by V, Cr, and Mn," *International Symposium on Metal-Hydrogen Systems*, Uppsala, Sweden.